Bright, dark, periodic and kink solitary wave solutions of evolutionary Zoomeron equation

Ghazala Akram[*], Maasoomah Sadaf[†] and Iqra Zainab[‡],
Department of Mathematics, University of the Punjab,
Quaid-e-Azam Campus, Lahore-54590, Pakistan.

Abstract

The modified auxiliary equation (MAE) approach and the generalized projective Riccati equation (GPRE) method are used to solve the Zoomeron problem in this study. Different types of exact traveling wave solutions are achieved, including solitary wave, periodic wave, bright, dark peakon, and kink-type wave solutions. Earned results are given as hyperbolic and trigonometric functions. Moreover, the dynamical features of obtained results are demonstrated through interesting plots.

Keywords: Nonlinear evolution equations; Zoomeron equation; Modified auxiliary equation method; Generalized projective Riccati equation method; Exact solutions.

1 Introduction

Nonlinear evolution equations (NLEEs) have been studied in a variety of mathematical-physical disciplines, including physics, biology, and chemistry. As, NLEEs define a large number of mathematical-physical models therefore, analytical solutions to these equations are significant [1, 2, 3]. Among many potential solutions to NLEEs, some special form solutions, such as solitons, may rely just on a single combination of variables [4, 5]. A soliton is a self-reinforcing solitary wave, also known as a wave packet or pulse, in mathematics and physics, which keeps its form while moving at a consistent rate. Solitons are created when nonlinear and dispersive effects in the medium cancel out.
The nonlinear evolutionary Zoomeron equation is the focus of this research. Calogero and Degasperis introduced the basic Zoomeron equation. They achieved a breakthrough in 1976 when they examined at one-dimensional Schrödinger equation and an extension of the well-known KdV equation to show solitons that travel at different speeds and discovered a link between their polarization effects and speed. This resulted in two forms of solitons: first defined as an accelerated soliton that arrived from one side in the far past and boomeranged back to the same side with same speed in the distant future. Second was a trapped soliton, oscillating in space about a fixed point with changing direction multiple times. The first

[*]toghazala2003@yahoo.com
[†]maasoomah.math@pu.edu.pk
[‡]iqrazainab40@gmail.com

one was named as Boomeron and second as Trappon. Consequently, the classical Zoomeron equation was derived. The Zoomeron equation therefore covers unique examples of solitons with distinct properties that emerge in a variety of physical situations, including laser physics, fluid dynamics and nonlinear optics. Consider the following nonlinear $(2+1)$-dimensional Zoomeron equation

$$\left(\frac{\Lambda_{xy}}{\Lambda}\right)_{tt} - \left(\frac{\Lambda_{xy}}{\Lambda}\right)_{xx} + 2(\Lambda^2)_{xt}, \tag{1}$$

where $\Lambda(x, y, t)$ is the magnitude of the corresponding wave mode. The presented model is one of the incognito evolution equation and has been explored via different direct approaches some important ones are, (G'/G)-expansion method [6], extended direct algebraic technique [7], sine-cosine function method [8], the extended $\exp(-\phi(\xi))$-expansion technique and exponential rational function technique [9], the exp-function method and modified simple equation method[10], the new Jacobi elliptic function expansion method, the exponential rational function method and Jacobi elliptic function rational expansion method [11], auxiliary equation method [12] and modified Kudryashov method [13]. Porsezian assured that the Zoomeron equation passes the P-property of integrability [14], Gandarias *et al.* examined symmetry and verified conservation laws [15] and Baleanu *et al.* presented it's stability analysis [16]. In this work, the modified auxiliary equation (MAE) method [17] and the generalized projective Riccati equation (GPRE) method [18] are for the first time being employed to acquire analytical solutions for the governing model. These methods are easy to proceed and provide reliable results.
The work is organized as follows: In Section 2 brief description of mentioned techniques is provided. Section 3 elaborates the earned results of Zoomeron equation via MAE method while in Section 4 exact solutions are derived with the help of generalized projective Riccati equation method. Section 5 contains discussion about obtained solutions and in Section 6 overall conclusion is drawn.

2 Description of proposed technique

The NLEE is considered, as

$$L(\Lambda, \Lambda_x, \Lambda_t, \Lambda_{xx}, \Lambda_{xt}, ...) = 0, \tag{2}$$

where $\Lambda = \Lambda(x, t)$ satisfies the NLEE (2).
Inserting the transformation

$$\Lambda(x, t) = \zeta(\Omega), \quad \Omega = x + by - ct. \tag{3}$$

Eq. (2) can be turned into an ODE, as

$$M(\zeta, \zeta', \zeta'', ...) = 0, \tag{4}$$

where b and c are real constants and $\zeta' = \frac{d\zeta}{d\Omega}$.

2.1 Modified auxiliary equation method

The MAE method assumes the general solution of Eq.(4), as

$$\zeta(\Omega) = \alpha_0 + \sum_{i=1}^{N} \left[\alpha_i (z^h)^i + \beta_i (z^h)^{-i}\right], \tag{5}$$

where α_is, β_is are constants to be calculated and $h(\Omega)$ follows the auxiliary equation

$$h'(\Omega) = \frac{\beta + \alpha z^{-h} + \gamma z^h}{lnz}. \tag{6}$$

Here α, β, γ and z are arbitrary constants with $z > 0,\ z \neq 1$. Further, α_is and β_is cannot be zero simultaneously and positive integer N can be computed by utilizing homogeneous balance principle (HBP) [19]. The solutions of Eq.(6) are as follows :

• If $\beta^2 - 4\alpha\gamma < 0$ and $\gamma \neq 0$,

$$z^{h(\Omega)} = \frac{-\beta + \sqrt{4\alpha\gamma - \beta^2}\tan(\frac{\sqrt{4\alpha\gamma-\beta^2}\Omega}{2})}{2\gamma} \quad \text{or} \quad z^{h(\Omega)} = -\frac{\beta + \sqrt{4\alpha\gamma - \beta^2}\cot(\frac{\sqrt{4\alpha\gamma-\beta^2}\Omega}{2})}{2\gamma}.$$

• If $\beta^2 - 4\alpha\gamma > 0$ and $\gamma \neq 0$,

$$z^{h(\Omega)} = -\frac{\beta + \sqrt{\beta^2 - 4\alpha\gamma}\tanh(\frac{\sqrt{\beta^2-4\alpha\gamma}\Omega}{2})}{2\gamma} \quad \text{or} \quad z^{h(\Omega)} = -\frac{\beta + \sqrt{\beta^2 - 4\alpha\gamma}\coth(\frac{\sqrt{\beta^2-4\alpha\gamma}\Omega}{2})}{2\gamma}.$$

• If $\beta^2 - 4\alpha\gamma = 0$ and $\gamma \neq 0$,

$$z^{h(\Omega)} = -\frac{2 + \beta\Omega}{2\gamma\Omega}.$$

2.2 Generalized projective Riccati equation method

The GPRE method assumes the general solution of Eq.(4), as

$$\zeta(\Omega) = A_0 + \sum_{i=1}^{N} \sigma^{i-1}(\Omega)\left[A_i\sigma(\Omega) + B_i\varrho(\Omega)\right], \tag{7}$$

where A_is and B_is are constants to be determined later. The functions $\sigma(\Omega)$ and $\varrho(\Omega)$ satisfy the ODEs

$$\begin{aligned} \sigma'(\Omega) &= \epsilon\sigma(\Omega)\varrho(\Omega), \\ \varrho'(\Omega) = K + \epsilon\varrho^2(\Omega) - \mu\sigma(\Omega), &\qquad \epsilon = \pm 1, \end{aligned} \tag{8}$$

such that

$$\varrho^2(\Omega) = -\epsilon\left[K - 2\mu\sigma(\Omega) + \frac{\mu^2 - 1}{K}\sigma^2(\Omega)\right], \tag{9}$$

where K and μ are arbitrary constants.
If $K = \mu = 0$, Eq.(4) has general solution, as

$$\zeta(\Omega) = \sum_{i=0}^{N} A_i\varrho^i(\Omega). \tag{10}$$

where $\varrho(\Omega)$ satisfies the ODE

$$\varrho'(\Omega) = \varrho^2(\Omega). \tag{11}$$

The positive integer N can be computed by utilizing homogeneous balance principle (HBP) [19]. Eq.(8) satisfy the following results:
(i) If $\epsilon = -1$, K$\neq 0$,

$$\sigma_1 = \frac{R \sec h\left(\sqrt{K}\Omega\right)}{\mu \sec h\left(\sqrt{K}\Omega\right) + 1}, \qquad \varrho_1 = \frac{\sqrt{K} \tan h\left(\sqrt{K}\Omega\right)}{\mu \sec h\left(\sqrt{K}\Omega\right) + 1} \tag{12}$$

$$\sigma_2 = \frac{K \csc h\left(\sqrt{K}\Omega\right)}{\mu \csc h\left(\sqrt{K}\Omega\right) + 1}, \qquad \varrho_2 = \frac{\sqrt{K} \cot h\left(\sqrt{K}\Omega\right)}{\mu \csc h\left(\sqrt{K}\Omega\right) + 1} \tag{13}$$

(ii) If $\epsilon = 1$, K$\neq 0$,

$$\sigma_3 = \frac{K \sec\left(\sqrt{K}\Omega\right)}{\mu \sec\left(\sqrt{K}\Omega\right) + 1}, \qquad \varrho_3 = \frac{\sqrt{K} \tan\left(\sqrt{K}\Omega\right)}{\mu \sec\left(\sqrt{K}\Omega\right) + 1} \tag{14}$$

$$\sigma_4 = \frac{K \csc\left(\sqrt{K}\Omega\right)}{\mu \csc\left(\sqrt{K}\Omega\right) + 1}, \qquad \varrho_4 = -\frac{\sqrt{K} \cot\left(\sqrt{K}\Omega\right)}{\mu \csc\left(\sqrt{K}\Omega\right) + 1} \tag{15}$$

(iii) If $K = \mu = 0$,

$$\sigma_5 = \frac{c_1}{\Omega}, \qquad \varrho_5 = \frac{1}{\epsilon\,\Omega}. \tag{16}$$

3 Exact solutions of governing model via modified auxiliary equation method

Considering the traveling wave transformation (3), where c represents speed of wave, in Eq.(1) and integrating it twice, gives

$$b(c^2 - 1)\zeta'' - 2c\zeta^3 - d\zeta = 0, \tag{17}$$

where d is taken as first constant of integration and second constant of integration is taken as zero. In accordance with HBP, maintaining a balance between ζ'' and ζ^3, gives $N = 1$. Then the following relation is obtained from Eq.(5)

$$\zeta(\Omega) = \alpha_0 + \alpha_1 z^h + \beta_1 z^{-h}. \tag{18}$$

Using Eq.(18) along with Eq.(6) in Eq.(17) and equating coefficients of each power of z^h to zero, provides the system of algebraic equations. The possible solutions of that system are

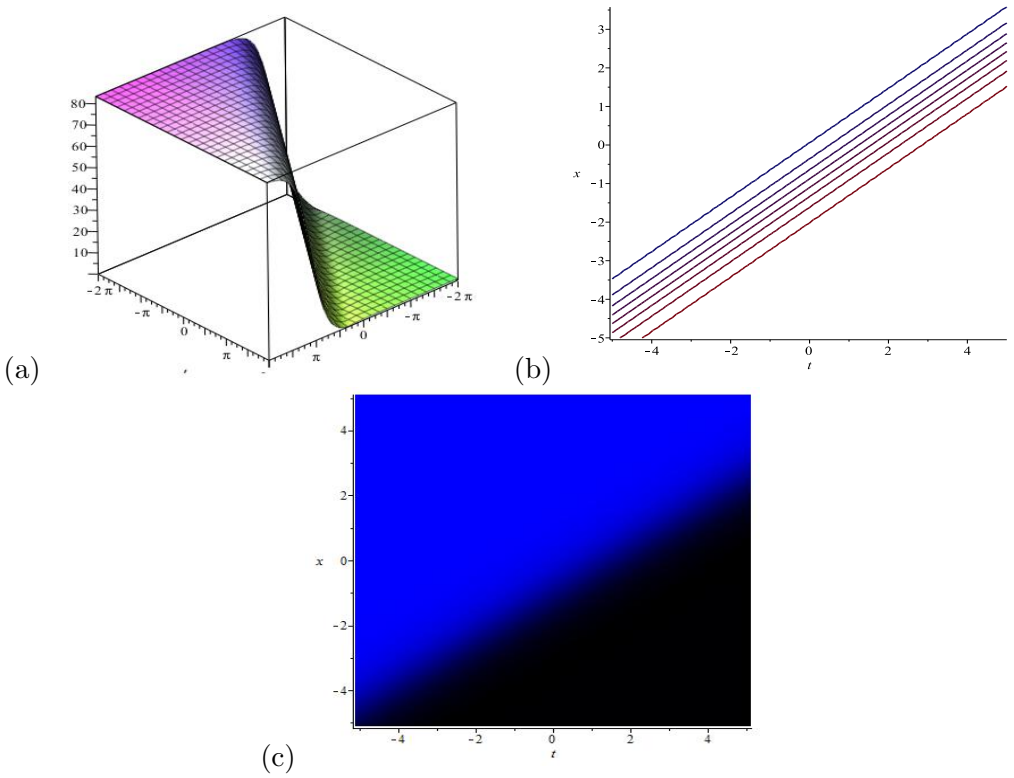

Figure 1: Graphical illustration of $|\Lambda_{1,3}(x,t)|$ with (a) $\alpha = 0.2,\ \beta = 2,\ \gamma = 0.02,\ b = 1,\ d = 1,\ y = 1$, (b) corresponding contour graph and (c) 2D-density plot.

retrieved with the help of Maple software, as

$$\textbf{Family1}: \quad \left[\alpha_0 = 1/2\,\frac{\beta\sqrt{2d}}{\sqrt[4]{(4\,\alpha\,\gamma-\beta^2)(4\,\alpha\,b\gamma-b\beta^2+2\,d)}},\right. \tag{19}$$
$$\left.\alpha_1 = \sqrt{2d}\sqrt[4]{\frac{b}{(4\,\alpha\,\gamma-\beta^2)(4\,\alpha\,b\gamma-b\beta^2+2\,d)}},\ \beta_1 = 0,\ c = \sqrt{\frac{4\,\alpha\,b\gamma-b\beta^2+2\,d}{4\,\alpha\,b\gamma-b\beta^2}}\right]$$

$$\textbf{Family2}: \quad \left[\alpha_0 = 1/2\,\frac{\beta\sqrt{2d}}{\sqrt[4]{(4\,\alpha\,\gamma-\beta^2)(4\,\alpha\,b\gamma-b\beta^2+2\,d)}},\right. \tag{20}$$
$$\left.\alpha_1 = 0,\ \beta_1 = \sqrt{2d}\sqrt[4]{\frac{b}{(4\,\alpha\,\gamma-\beta^2)(4\,\alpha\,b\gamma-b\beta^2+2\,d)}},\ c = \sqrt{\frac{4\,\alpha\,b\gamma-b\beta^2+2\,d}{4\,\alpha\,b\gamma-b\beta^2}}\right]$$

Family1 $\beta^2 - 4\alpha\gamma < 0$ and $\gamma \neq 0$, provide

$$\begin{aligned}\Lambda_{1,1}(x,t) &= \frac{\beta\sqrt{2d}}{2\sqrt[4]{(4\,\alpha\,\gamma-\beta^2)\,(4\,\alpha\,b\gamma-b\beta^2+2\,d)}} \\ &+\sqrt{2d}\sqrt[4]{\frac{b}{(4\,\alpha\,\gamma-\beta^2)\,(4\,\alpha\,b\gamma-b\beta^2+2\,d)}} \\ &\times\left(\frac{-\beta+\sqrt{4\alpha\gamma-\beta^2}\tan(\frac{\sqrt{4\alpha\gamma-\beta^2}\Omega}{2})}{2\gamma}\right) \end{aligned} \tag{21}$$

or

$$\begin{aligned}\Lambda_{1,2}(x,t) &= \frac{\beta\sqrt{2d}}{2\sqrt[4]{(4\,\alpha\,\gamma-\beta^2)\,(4\,\alpha\,b\gamma-b\beta^2+2\,d)}} \\ &-\sqrt{2d}\sqrt[4]{\frac{b}{(4\,\alpha\,\gamma-\beta^2)\,(4\,\alpha\,b\gamma-b\beta^2+2\,d)}} \\ &\times\left(\frac{\beta+\sqrt{4\alpha\gamma-\beta^2}\cot(\frac{\sqrt{4\alpha\gamma-\beta^2}\Omega}{2})}{2\gamma}\right). \end{aligned} \tag{22}$$

$\beta^2 - 4\alpha\gamma > 0$ and $\gamma \neq 0$, give

$$\begin{aligned}\Lambda_{1,3}(x,t) &= \frac{\beta\sqrt{2d}}{2\sqrt[4]{(4\,\alpha\,\gamma-\beta^2)\,(4\,\alpha\,b\gamma-b\beta^2+2\,d)}} \\ &-\sqrt{2d}\sqrt[4]{\frac{b}{(4\,\alpha\,\gamma-\beta^2)\,(4\,\alpha\,b\gamma-b\beta^2+2\,d)}} \\ &\times\left(\frac{\beta+\sqrt{\beta^2-4\alpha\gamma}\tanh(\frac{\sqrt{\beta^2-4\alpha\gamma}\Omega}{2})}{2\gamma}\right) \end{aligned} \tag{23}$$

or

$$\begin{aligned}\Lambda_{1,4}(x,t) &= \frac{\beta\sqrt{2d}}{2\sqrt[4]{(4\,\alpha\,\gamma-\beta^2)\,(4\,\alpha\,b\gamma-b\beta^2+2\,d)}} \\ &-\sqrt{2d}\sqrt[4]{\frac{b}{(4\,\alpha\,\gamma-\beta^2)\,(4\,\alpha\,b\gamma-b\beta^2+2\,d)}} \\ &\times\left(\frac{\beta+\sqrt{\beta^2-4\alpha\gamma}\coth(\frac{\sqrt{\beta^2-4\alpha\gamma}\Omega}{2})}{2\gamma}\right). \end{aligned} \tag{24}$$

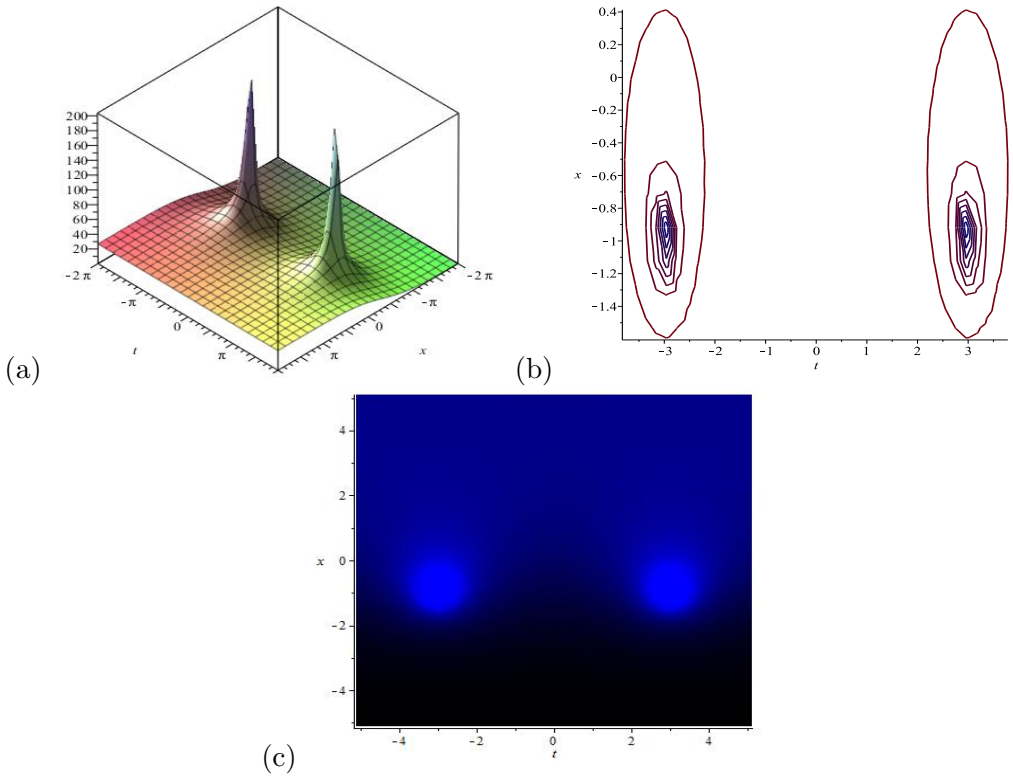

Figure 2: Graphical illustration of $|\Lambda_{1,3}(x,t)|$ with (a) $\alpha = 0.5,\ \beta = 1,\ \gamma = 0.05,\ b = 1,\ d = 1,\ y = 1$, (b) corresponding contour graph and (c) 2D-density plot.

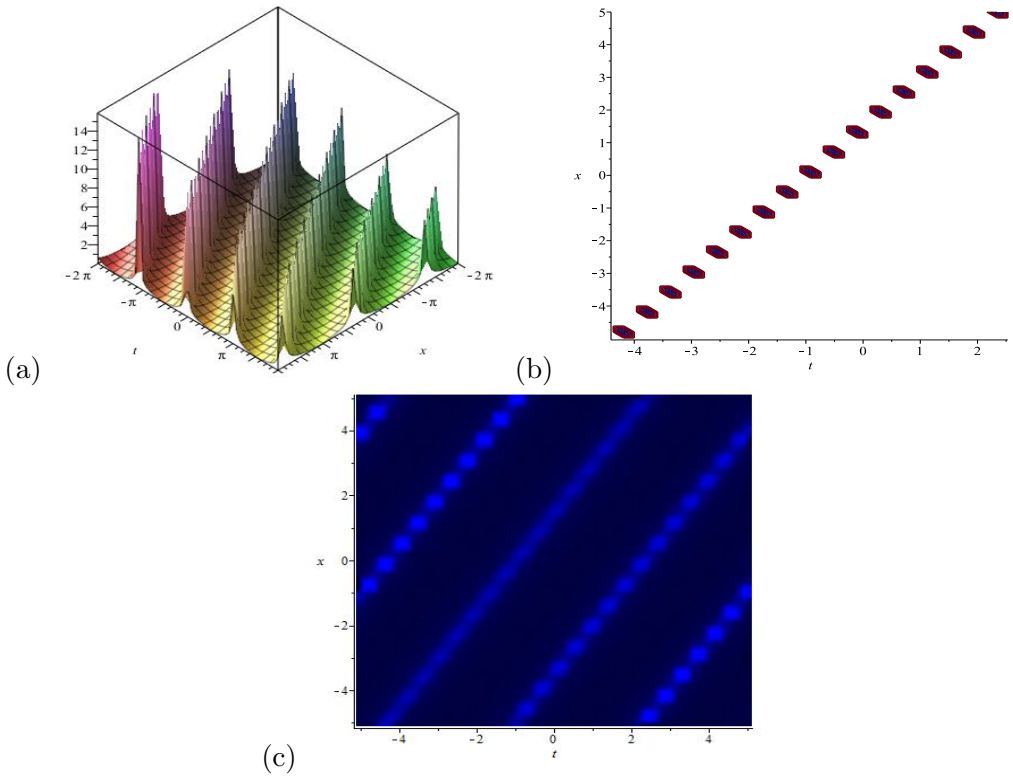

Figure 3: Graphical illustration of $|\Lambda_{2,2}(x,t)|$ with (a) $\alpha = 0.2,\ \beta = 2,\ \gamma = 0.02,\ b = 1,\ d = 1,\ y = 1$, (b) corresponding contour graph and (c) 2D-density plot.

Family2 $\beta^2 - 4\alpha\gamma < 0$ and $\gamma \neq 0$, provide

$$\begin{aligned}\Lambda_{2,1}(x,t) &= \frac{\beta\sqrt{2d}}{2\sqrt[4]{(4\,\alpha\,\gamma-\beta^2)\,(4\,\alpha\,b\gamma-b\beta^2+2\,d)}} \\ &+\sqrt{2d}\sqrt[4]{\frac{b}{(4\,\alpha\,\gamma-\beta^2)\,(4\,\alpha\,b\gamma-b\beta^2+2\,d)}} \\ &\times\left(\frac{-\beta+\sqrt{4\alpha\gamma-\beta^2}\tan(\frac{\sqrt{4\alpha\gamma-\beta^2}\Omega}{2})}{2\gamma}\right)^{-1} \end{aligned} \tag{25}$$

or

$$\begin{aligned}\Lambda_{2,2}(x,t) &= \frac{\beta\sqrt{2d}}{2\sqrt[4]{(4\,\alpha\,\gamma-\beta^2)\,(4\,\alpha\,b\gamma-b\beta^2+2\,d)}} \\ &-\sqrt{2d}\sqrt[4]{\frac{b}{(4\,\alpha\,\gamma-\beta^2)\,(4\,\alpha\,b\gamma-b\beta^2+2\,d)}} \\ &\times\left(\frac{\beta+\sqrt{4\alpha\gamma-\beta^2}\cot(\frac{\sqrt{4\alpha\gamma-\beta^2}\Omega}{2})}{2\gamma}\right)^{-1}. \end{aligned} \tag{26}$$

$\beta^2 - 4\alpha\gamma > 0$ and $\gamma \neq 0$, give

$$\begin{aligned}\Lambda_{2,3}(x,t) &= \frac{\beta\sqrt{2d}}{2\sqrt[4]{(4\,\alpha\,\gamma-\beta^2)\,(4\,\alpha\,b\gamma-b\beta^2+2\,d)}} \\ &-\sqrt{2d}\sqrt[4]{\frac{b}{(4\,\alpha\,\gamma-\beta^2)\,(4\,\alpha\,b\gamma-b\beta^2+2\,d)}} \\ &\times\left(\frac{\beta+\sqrt{\beta^2-4\alpha\gamma}\tanh(\frac{\sqrt{\beta^2-4\alpha\gamma}\Omega}{2})}{2\gamma}\right)^{-1} \end{aligned} \tag{27}$$

or

$$\begin{aligned}\Lambda_{2,4}(x,t) &= \frac{\beta\sqrt{2d}}{2\sqrt[4]{(4\,\alpha\,\gamma-\beta^2)\,(4\,\alpha\,b\gamma-b\beta^2+2\,d)}} \\ &-\sqrt{2d}\sqrt[4]{\frac{b}{(4\,\alpha\,\gamma-\beta^2)\,(4\,\alpha\,b\gamma-b\beta^2+2\,d)}} \\ &\times\left(\frac{\beta+\sqrt{\beta^2-4\alpha\gamma}\coth(\frac{\sqrt{\beta^2-4\alpha\gamma}\Omega}{2})}{2\gamma}\right)^{-1}. \end{aligned} \tag{28}$$

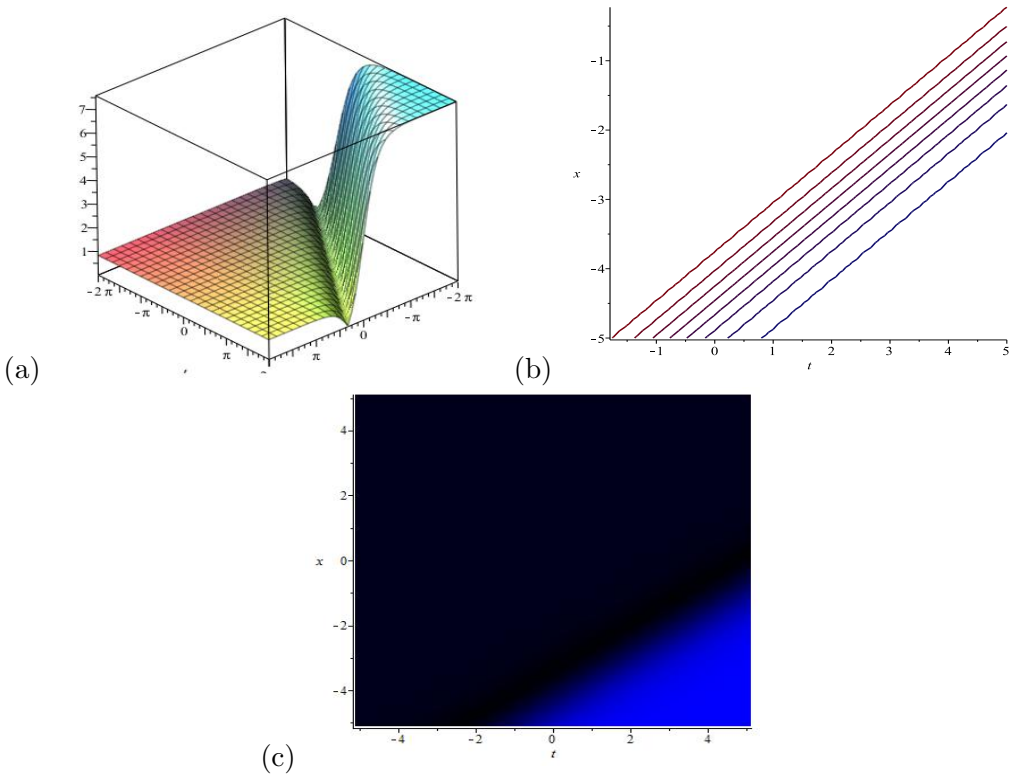

Figure 4: Graphical illustration of $|\Lambda_{2,3}(x,t)|$ with (a) $\alpha = 0.2,\ \beta = 2,\ \gamma = 0.02,\ b = 1,\ d = 1,\ y = 1$, (b) corresponding contour graph and (c) 2D-density plot.

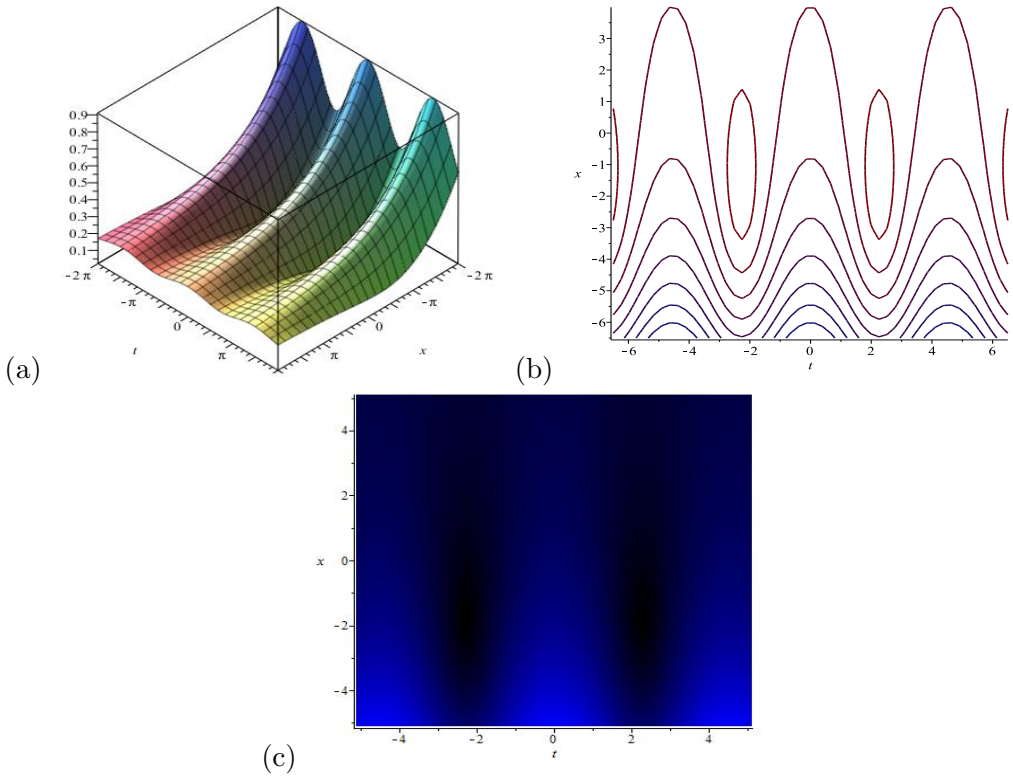

Figure 5: Graphical illustration of $|\Lambda_{2,4}(x,t)|$ for with (a) $\alpha = 0.03,\ \beta = 0.3,\ \gamma = 0.02,\ b = 1,\ d = 1,\ y = 1$, (b) corresponding contour graph and (c) 2D-density plot.

4 Exact solutions of governing model via generalized projective Riccati equation method

The GPRE method assumes general solution of ODE (17) for $N = 1$, as

$$\zeta(\Omega) = A_0 + A_1\sigma(\Omega) + B_1\varrho(\Omega). \tag{29}$$

Using Eq.(29) along with Eq.(8) in Eq.(17) and equating coefficients of $\sigma^i(\Omega)\varrho^j(\Omega)$, where $(i = 0, 1, 2, ..., j = 0, 1.)$, to zero provides the system of algebraic equations. The possible solutions of that system are retrieved with the help of Maple software, as

$$\textbf{Family1}: \quad \left[A_0 = 0,\ A_1 = 0,\ B_1 = \sqrt[4]{-\tfrac{-2\,bd^2\epsilon^2+bd^2}{8\,R^2b\epsilon^4-4\,K^2b\epsilon^2+8\,Kd\epsilon}},\ \mu = \pm 1,\ c = \tfrac{\sqrt{2\,Kb\epsilon^3-Kb\epsilon+2\,d}}{\sqrt{K\epsilon\,b(2\,\epsilon^2-1)}}\right]$$

$$\textbf{Family2}: \quad \left[A_0 = 0,\ A_1 = 0,\ B_1 = \sqrt[4]{\tfrac{bd^2\epsilon}{4\,K^2b\epsilon^3+2\,Kd}},\ \mu = 0,\ c = 1/2\,\tfrac{\sqrt{2\,Kb\epsilon^3+d}\sqrt{2}}{\sqrt{bK\epsilon\epsilon}}\right]$$

$$\textbf{Family3}: \quad \left[A_0 = 0,\ A_1 = \sqrt{-\tfrac{bd\epsilon}{K\sqrt{Kb\epsilon\,(2\,\epsilon^2-1)(2\,Kb\epsilon^3-Kb\epsilon-d)}}}\epsilon,\ B_1 = 0,\ \mu = 0,\ c = \sqrt{\tfrac{2\,Kb\epsilon^3-Kb\epsilon-d}{2\,Kb\epsilon^3-Kb\epsilon}}\right]$$

Family1 $\epsilon = -1$ and $K \neq 0$, provide

$$\Lambda_{1,1}(x,t) = \sqrt[4]{-\frac{-2\,bd^2+bd^2}{8\,K^2b-4\,K^2b-8\,Kd}}\left(\frac{\sqrt{K}\tan h\left(\sqrt{K}\Omega\right)}{1\pm\sec h\left(\sqrt{K}\Omega\right)}\right) \tag{30}$$

and

$$\Lambda_{1,2}(x,t) = \sqrt[4]{-\frac{-2\,bd^2+bd^2}{8\,K^2b-4\,K^2b-8\,Kd}}\left(\frac{\sqrt{K}\cot h\left(\sqrt{K}\Omega\right)}{1\pm\csc h\left(\sqrt{K}\Omega\right)}\right). \tag{31}$$

$\epsilon = 1$ and $K \neq 0$, provide

$$\Lambda_{1,3}(x,t) = \sqrt[4]{-\frac{-2\,bd^2+bd^2}{8\,K^2b-4\,K^2b+8\,Kd}}\left(\frac{\sqrt{K}\tan\left(\sqrt{K}\Omega\right)}{1\pm\sec\left(\sqrt{K}\Omega\right)}\right) \tag{32}$$

and

$$\Lambda_{1,4}(x,t) = \sqrt[4]{-\frac{-2\,bd^2+bd^2}{8\,K^2b-4\,K^2b+8\,Kd}}\left(-\frac{\sqrt{K}\cot\left(\sqrt{K}\Omega\right)}{1\pm\csc\left(\sqrt{K}\Omega\right)}\right). \tag{33}$$

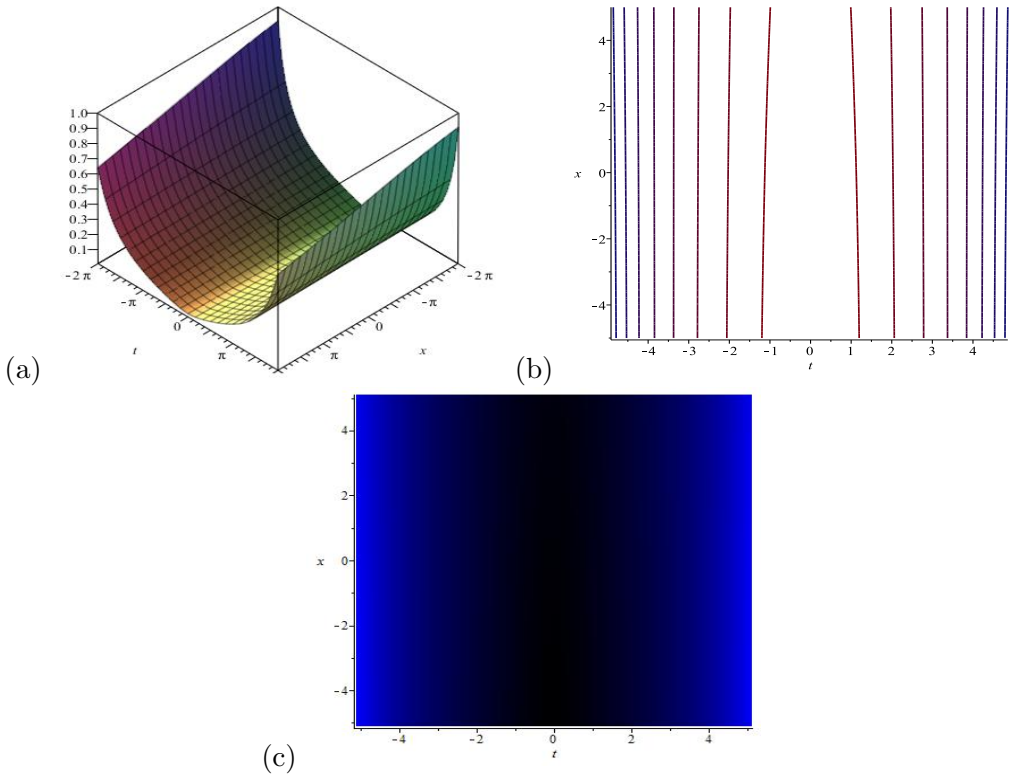

Figure 6: Graphical illustration of $|\Lambda_{1,1}(x,t)|$ with (a)$K = 0.0005,\ b = 10,\ d = 1,\ y = 1,$ (b) corresponding contour graph and (c) 2D-density plot.

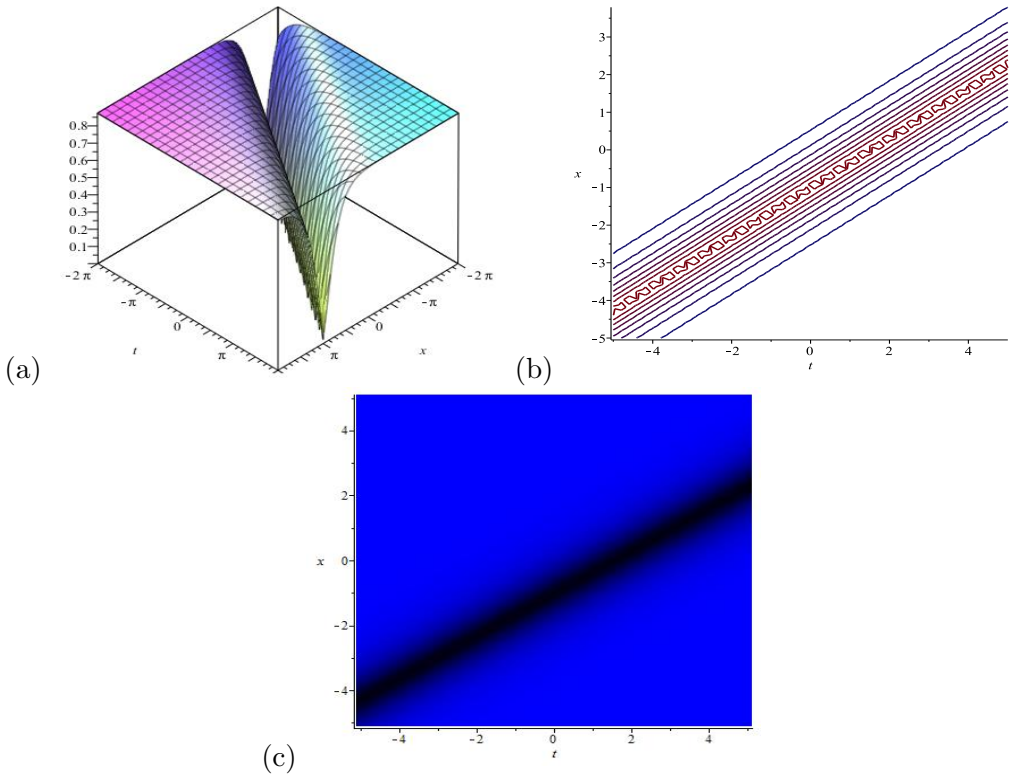

Figure 7: Graphical illustration of $|\Lambda_{1,1}(x,t)|$ with (a)$K = 3.5,\ b = 1,\ d = 1,\ y = 1$, (b) corresponding contour graph and (c) 2D-density plot.

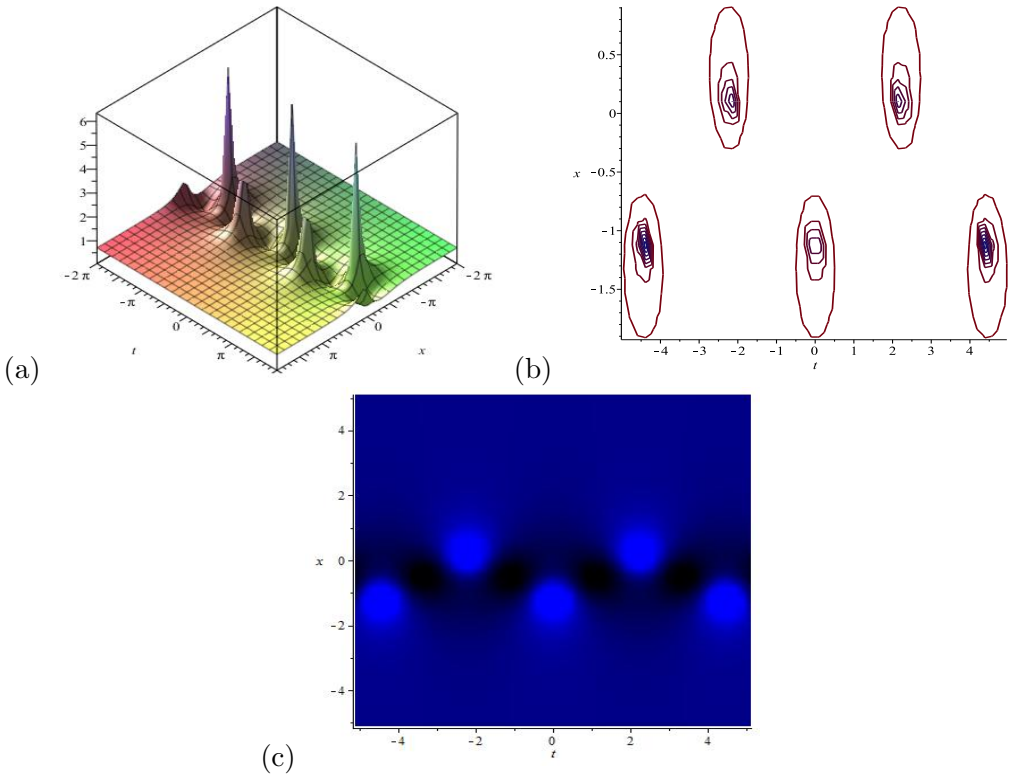

Figure 8: Graphical illustration of $|\Lambda_{1,2}(x,t)|$ with (a)$K = 2,\ b = 0.5,\ d = 1,\ y = 1$, (b) corresponding contour graph and (c) 2D-density plot.

Family2 $\epsilon = -1$ and $K \neq 0$, provide

$$\Lambda_{2,1}(x,t) = \left(\sqrt{K}\tan h\left(\sqrt{K}\Omega\right)\right)\sqrt[4]{\frac{-bd^2}{-4\,K^2b+2\,Kd}} \tag{34}$$

and

$$\Lambda_{2,2}(x,t) = \left(\sqrt{K}\cot h\left(\sqrt{K}\Omega\right)\right)\sqrt[4]{\frac{-bd^2}{-4\,K^2b+2\,Kd}}. \tag{35}$$

$\epsilon = 1$ and $K \neq 0$, provide

$$\Lambda_{2,3}(x,t) = \left(\sqrt{K}\tan\left(\sqrt{K}\Omega\right)\right)\sqrt[4]{\frac{bd^2}{4\,K^2b+2\,Kd}} \tag{36}$$

and

$$\Lambda_{2,4}(x,t) = \left(-\sqrt{K}\cot\left(\sqrt{K}\Omega\right)\right)\sqrt[4]{\frac{bd^2}{4\,K^2b+2\,Kd}}\sigma_1 = \frac{K\sec h\left(\sqrt{K}\Omega\right)}{\mu\sec h\left(\sqrt{K}\Omega\right)+1}. \tag{37}$$

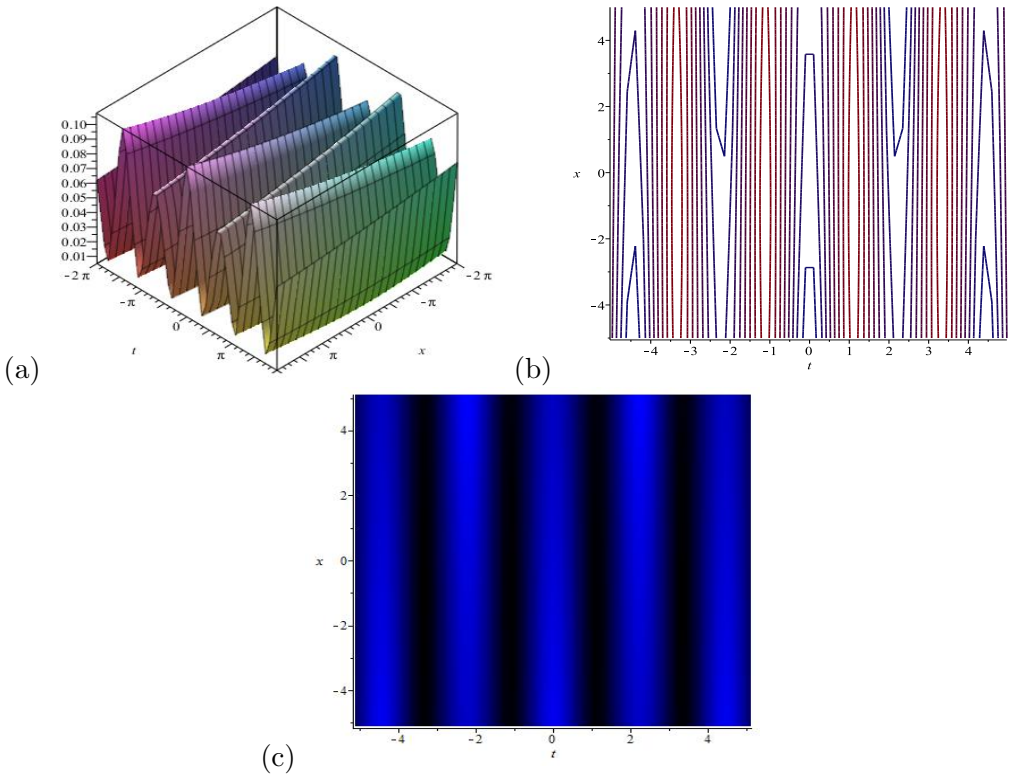

Figure 9: Graphical illustration of $|\Lambda_{1,2}(x,t)|$ with (a)$K = 0.0005,\ b = 1,\ d = 1,\ y = 1$, (b) corresponding contour graph and (c) 2D-density plot.

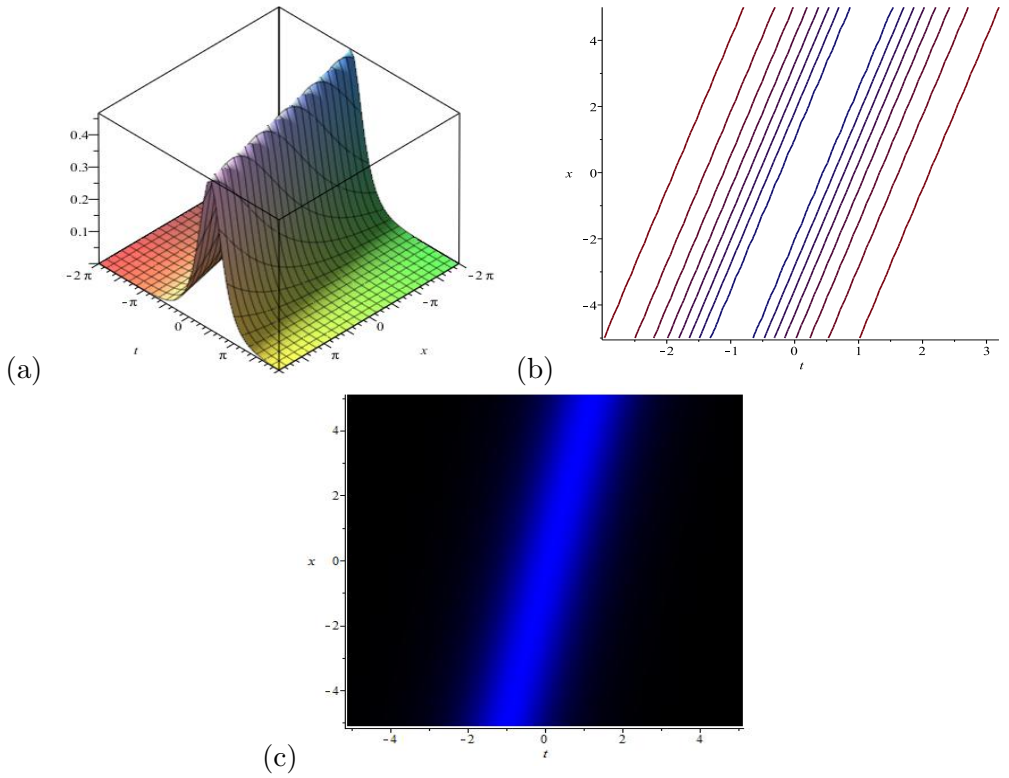

Figure 10: Graphical illustration of $|\Lambda_{3,1}(x,t)|$ with (a)$K = 0.1,\ b = 0.5,\ d = 1,\ y = 1$, (b) corresponding contour graph and (c) 2D-density plot.

Family3 $\epsilon = -1$ and $K \neq 0$, provide

$$\Lambda_{3,1}(x,t) = -\sqrt{\frac{bd}{K\sqrt{Kb\ (Kb+d)}}}\left(K \sec h\left(\sqrt{K}\Omega\right)\right) \tag{38}$$

and

$$\Lambda_{3,2}(x,t) = -\sqrt{\frac{bd}{K\sqrt{Kb\ (Kb+d)}}}\left(K \csc h\left(\sqrt{K}\Omega\right)\right). \tag{39}$$

$\epsilon = 1$ and $K \neq 0$, provide

$$\Lambda_{3,3}(x,t) = \sqrt{-\frac{bd}{K\sqrt{Kb\ (Kb-d)}}}\left(K \sec\left(\sqrt{K}\Omega\right)\right) \tag{40}$$

and

$$\Lambda_{3,4}(x,t) = \sqrt{-\frac{bd}{K\sqrt{Kb\ (Kb-d)}}}\left(K \csc\left(\sqrt{K}\Omega\right)\right). \tag{41}$$

5 Graphical Explanation

The traveling patterns of obtained solutions are presented as 3D surface plots. For some graphs it is easy to observe variations in 3D surface graphics through contours and density plots. That's why corresponding to each 3D pattern, contours and density graphs are plotted. Fig-[1] represents absolute 3D plot of solution of the Eq.(23) corresponding to the set of parameter values $\alpha = 0.2,\ \beta = 2,\ \gamma = 0.02,\ b = 1$ and $d = 1$ at $y = 1$. For these selected values of parameters kink solitary wave is observed. For $\alpha = 0.5,\ \beta = 1,\ \gamma = 0.05,\ b = 1$ and $d = 1$ at $y = 1$ a different solitary wave pattern is observed in Fig-[2]. Fig-[3] represents absolute 3D plot of solution of the Eq.(26) corresponding to the set of parameter values $\alpha = 0.2,\ \beta = 2,\ \gamma = 0.02,\ b = 1$ and $d = 1$ at $y = 1$. For these selected values of parameters periodic behavior is observed. Fig-[4] and Fig-[5] represent two different solitary wave patterns corresponding to Eq.(27) and Eq.(28) for selected set of parameter values $\alpha = 0.2,\ \beta = 2,\ \gamma = 0.02,\ b = 1,\ d = 1$ and $\alpha = 0.03,\ \beta = 0.3,\ \gamma = 0.02,\ b = 1,\ d = 1$ at $y = 1$, respectively. Fig-[6] represents absolute 3D plot of solution of the Eq.(30) corresponding to the set of parameter values $K = 0.0005,\ b = 10,\ d = 1$ at $y = 1$. For these selected values of parameters a new travelling pattern is observed. For $K = 3.5,\ b = 1$ and $d = 1$ at $y = 1$ a dark peakon wave is observed in Fig-[7]. Fig-[8] represents absolute 3D plot of solution of the Eq.(31) corresponding to the set of parameter values $K = 2,\ b = 0.5$ and $d = 1$ at $y = 1$. For these selected values of parameters a different solitary wave pattern is observed. For $K = 0.0005,\ b = 1$ and $d = 1$ at $y = 1$ a periodic wave is observed in Fig-[9]. Fig-[10] represents absolute 3D plot of solution of the Eq.(38) corresponding to the set of parameter values $K = 0.1,\ b = 0.5$ and $d = 1$ at $y = 1$. For these selected values of parameters bright soliton is observed. Most of the mentioned patterns are new and rest of them are in accordance with graphs already available in literature.

6 Conclusion

This attempt culminated in successful investigation of the evolutionary Zoomeron equation via modified auxiliary equation approach and generalized projective Riccati equation method. The obtained results are consistent with those previously available in literature, indicating that the suggested approaches are reliable. The set of achieved results includes kink, periodic, dark peakon, bright solitons and different solitary wave solutions. These solutions are presented as trigonometric and hyperbolic functions. The obtained solutions showed a complex behavior characterized by the constraints of proposed methodologies. The achieved complex behaviors as presented in Fig-[5], Fig-[7] and Fig-[9] are new one and not reported earlier for the governing model. In addition, the provided study identifies several intriguing patterns that will be helpful in analyzing nature of the model solutions as well as the consequences of the indicated approaches in the future.

References

[1] N. Faraz, M. Sadaf, G. Akram, I. Zainab, and Y. Khan. Effects of fractional order time derivative on the solitary wave dynamics of the generalized ZK-Burgers equation. *Results in Physics*, 25:104217, 2021.

[2] G. Akram, M. Sadaf, M. Sarfraz, and N. Anum. Dynamics investigation of (1+1)-dimensional time-fractional potential Korteweg-de Vries equation. *Alexandria Engineering Journal*, 61(1):501–509, 2022.

[3] G. Akram, M. Sadaf, M. Abbas, I. Zainab, and S.R. Gillani. Efficient techniques for traveling wave solutions of time-fractional Zakharov-Kuznetsov equation. *Mathematics and Computers in Simulation*, 193:607–622, 2022.

[4] G. Akram and N. Mahak. The modified auxiliary equation method to investigate solutions of the perturbed nonlinear Schrödinger equation with kerr law nonlinearity. *International Journal for Light and Electron Optics*, 207:164467, 2020.

[5] G. Akram, M. Sadaf, M. Dawood, and D. Baleanu. Optical solitons for Lakshmanan-Porsezian-Daniel equation with kerr law non-linearity using improved $\tan\psi(\eta)2$-expansion technique. *Results in Physics*, 29:104758, 2021.

[6] R. Abazari. The solitary wave solutions of Zoomeron equation. *Applied Mathematical Sciences*, 5(59):2943–2949, 2011.

[7] W. Gao, H. Rezazadeh, Z. Pinar, H.M. Baskonus, S. Sarwar, and G. Yel. Novel explicit solutions for the nonlinear Zoomeron equation by using newly extended direct algebraic technique. *Optical and Quantum Electronics*, 52(1):1–13, 2020.

[8] A. Qawasmeh. Soliton solutions of (2+1)-Zoomeron equation and Duffing equation and SRLW equation. *Journal of Mathematical and Computational Science*, 3(6):1475–1480, 2013.

[9] D. Kumar and M. Kaplan. New analytical solutions of (2+1)-dimensional conformable time fractional Zoomeron equation via two distinct techniques. *Chinese journal of physics*, 56(5):2173–2185, 2018.

[10] K. Khan and M.A. Akbar. Traveling wave solutions of the (2+ 1)-dimensional Zoomeron equation and the Burgers equations via the MSE method and the Exp-function method. *Ain Shams Engineering Journal*, 5(1):247–256, 2014.

[11] E.T. Tebue, Z. Djoufack, A.D. Tsajio, and A.K. Jiotsa. Solitons and other solutions of the nonlinear fractional Zoomeron equation. *Chinese journal of physics*, 56(3):1232–1246, 2018.

[12] M. Topsakal and F. TaŞcan. Exact travelling wave solutions for space-time fractional Klein-Gordon equation and (2+ 1)-dimensional time-fractional Zoomeron equation via auxiliary equation method. *Applied Mathematics and Nonlinear Sciences*, 5(1):437–446, 2020.

[13] K. Hosseini, A. Korkmaz, A. Bekir, F. Samadani, A. Zabihi, and M. Topsakal. New wave form solutions of nonlinear conformable time-fractional Zoomeron equation in (2+ 1)-dimensions. *Waves in Random and Complex Media*, 31(2):228–238, 2021.

[14] K. Porsezian. Integrability aspects and soliton solutions of some field theoretical equations. *Physics Letters A*, 240(4-5):196–200, 1998.

[15] T. Motsepa, C.M. Khalique, and M.L. Gandarias. Symmetry analysis and conservation laws of the Zoomeron equation. *Symmetry*, 9(2):27, 2017.

[16] M. Inc, A. Yusuf, A.I. Aliyu, and D. Baleanu. Soliton solutions and stability analysis for some conformable nonlinear partial differential equations in mathematical physics. *Optical and Quantum Electronics*, 50(4):1–14, 2018.

[17] M.S. Osman, D. Lu, M.M.A. Khater, and R.A.M. Attia. Complex wave structures for abundant solutions related to the complex Ginzburg-Landau model. *International Journal for Light and Electron Optics*, 192:162927, 2019.

[18] E.M.E. Zayed and K.A.E. Alurrfi. The generalized projective Riccati equations method for solving nonlinear evolution equations in mathematical physics. *Abstract and Applied Analysis*, 2014, 2014.

[19] S. Sirisubtawee and S. Koonprasert. Exact traveling wave solutions of certain nonlinear partial differential equations using the $(\frac{G'}{G^2})$-expansion method. *Advances in Mathematical Physics*, 2018:1–15, 2018.